# Vibrationally Mediated Photodissociation of Jet-Cooled $CH_3CF_2Cl$: A Probe of Energy Flow and Bond Breaking Dynamics†

**Gabriela Dorfman, Aviva Melchior,* and Salman Rosenwaks**

*Department of Physics, Ben-Gurion University of the Negev, Beer-Sheva 84105, Israel*

**Ilana Bar**

*The Institutes for Applied Research, Ben-Gurion University of the Negev, Beer-Sheva 84105, Israel*

*Received: December 5, 2001; In Final Form: May 1, 2002*

A double resonance scheme was employed to photodissociate jet-cooled $CH_3CF_2Cl$ in a time-of-flight mass spectrometer. First, the molecule was promoted to the second ($3\nu_{CH}$) or third ($4\nu_{CH}$) methyl overtone by direct IR excitation. Subsequently, a UV laser beam at ∼235 nm was used to both dissociate the molecule and tag the Cl $^2P_{3/2}$ [Cl] and Cl $^2P_{1/2}$ [Cl*] photofragments by (2 + 1) resonantly enhanced multiphoton ionization. The photofragment action spectra revealed multiple peak structures in both overtone regions, attributed to couplings of the C−H stretches and to methyl stretch−deformation Fermi resonances. The cooling of the samples afforded narrowing of the peaks, relative to room temperature photoacoustic spectra, due to the reduced rotational and vibrational congestion, and enabled observation of a new splitting in the high frequency peak of the second overtone. This splitting apparently resulted from a local resonance of the mixed stretch−deformation state with a close lying dark state. The time scales for vibrational energy redistribution in the local resonance and between the mixed stretch−deformations were evaluated. These time scales and the measured Cl*/Cl branching ratios were compared to those of other hydrohalocarbon compounds. The Cl*/Cl ratio was also compared to that of the nearly isoenergetic vibrationless ground state 193 nm photodissociation and found to be different, demonstrating the effect of vibrational pre-excitation on the photodissociation dynamics.

## Introduction

Vibrationally mediated photodissociation (VMP),[1,2] where vibrationally pre-excited molecules are further excited to a dissociative electronic state, is an advantageous tool in exploration of both photolysis dynamics and vibrational spectroscopy. In VMP, the wave function of the vibrationally excited molecule extends to wider portions of the ground state potential energy surface (PES), and therefore when promoted to upper PES(s) it samples different regions of it (them). This allows the manipulation, to some extent, of the photodissociation outcome. The vibrational pre-excitation may affect the photoproduct branching ratios and their quantum states, especially when more than one excited PES is involved and the adiabatic and nonadiabatic interplay between them is significant to the photodissociation process.[2−12]

Also, utilizing VMP with jet-cooled samples facilitates monitoring of action spectra, i.e., the photoproduct yield as a function of the vibrational excitation laser wavelength. These vibrational overtone spectra benefit from a reduced spectral congestion provided by relatively fewer populated rotational lines and the removal of hot bands, and from the signal enhancement originating from a better Franck−Condon (FC) overlap of the vibrational state with the upper PES. This affords diminishing of the inhomogeneous structure and revealing, in some cases, splittings caused by local resonances between the initially excited states and close lying states. Therefore, action spectra serve as a valuable source for information on the time scales of intramolecular vibrational redistribution (IVR) and the specific pathways of energy flow.[2−4,13−16]

The present work is an extension of our previous VMP research on hydrochlorofluorocarbon (HCFC) compounds.[3,4,15,17−19] These species are of atmospheric importance due to the phase out of the ozone destroying chlorofluorocarbons (CFCs) and halons[20−22] and their interim replacement by HCFCs. The HCFCs contain one or more C−H bonds and therefore are active toward OH and O($^1$D) free radicals in the troposphere. Consequently, their atmospheric lifetimes are shorter than those of fully halogenated CFCs and their ozone depletion potentials and global warming potentials are lower. Also, the first absorption band of the HCFCs (designated as the A band) in the 180−240 nm range[23] is of atmospheric relevance since photolytic decomposition through the middle and lower stratosphere (20−30 km) occurs predominantly in this spectral range.[24] In all HCFCs these bands are broad and unstructured, with absorption cross sections ($\sigma$) differing by several orders of magnitude in different molecules. Nevertheless, all compounds show the same trend of high $\sigma$ at short wavelengths, decreasing gradually toward the red wing.[24−26] This electronic transition can be described as a $\sigma^* \leftarrow n_{Cl}$ excitation, involving the promotion of an electron from a nonbonding Cl 2p orbital to an antibonding C−Cl orbital.[23]

We studied the ∼235/243 nm photodissociation of $CHFCl_2$ (HCFC 21) and $CHF_2Cl$ (HCFC 22) vibrationally excited to the $N$ = 3, 7/2, and 4 C−H stretch−bend polyads (see below),[15,17,18] and of $CH_3CFCl_2$ (HCFC 141b) excited to the

† Part of the special issue "Donald Setser Festschrift".

* Corresponding author.

10.1021/jp014431v CCC: $22.00 
Published on Web 06/22/2002

fundamental symmetric and the second and third overtones of the $CH_3$ stretch.[3,4,19] The VMP results were compared to the 193 nm photodissociation of vibrationless ground-state molecules.[7,27,28] The photodissociation of both vibrationless ground state and vibrationally excited molecules was characterized by extensive release of Cl photofragments occurring in both ground Cl $^2P_{3/2}$ [Cl] and spin−orbit excited Cl $^2P_{1/2}$ [Cl*] states and some loss of H atoms. Comparison of the action spectra of Cl, Cl*, and H with the room-temperature photoacoustic (PA) spectra, monitored simultaneously, revealed considerable narrowing of the former, enabling in some cases exposure of new features. Also, the yield of all photofragments increased relative to the vibrationless ground-state photodissociation at ∼235/243 nm, however, with a lesser extent for H, although the vibrational energy was deposited in the C−H stretches. The new features and the enhancement of the chlorine yield are indications of energy flow via anharmonic couplings to other vibrational modes. In the case of $CH_3CFCl_2$ the VMP Cl*/Cl branching ratio differed from that of the almost isoenergetic 193 nm direct photodissociation, showing that the involvement of the vibrational intermediate state affected the dynamics of the photodissociation.

Previously we also measured the room-temperature PA vibrational spectra in the second ($3\nu_{CH}$), third ($4\nu_{CH}$), and fourth ($5\nu_{CH}$) $CH_3$ overtones of $CH_3CF_2Cl$ (HCFC 142b) and found out that they were characterized by a multipeak structure that was attributed to strong coupling between the zeroth order C−H stretch and deformation states that generated the observed mixed eigenstates.[29] A simplified local mode (LM) model was used by us to assign the spectra. The LM model, based on the model of Duncan et al.,[30] included Darling−Dennison resonances between the C−H stretches and stretch−deformation Fermi resonances.[29] The present paper focuses on the ∼235 nm photodissociation of $CH_3CF_2Cl$ pre-excited to $3\nu_{CH}$ and $4\nu_{CH}$. By monitoring the more detailed jet-cooled action spectra, additional information and a better understanding of the processes controlling energy redistribution and their time scales was achieved. The influence of the initially prepared vibrational states on the access to the upper PESs and the nonadiabatic interactions between them was assessed by determining the Cl*/Cl branching ratio and comparing it to that in direct 193 nm photodissociation.

## Experimental Section

The concept of the experiments is illustrated in Figure 1. In the first stage the molecule was excited to the second or third $CH_3$ overtone of $CH_3CF_2Cl$ with an IR laser beam, then a second laser in the UV (∼235 nm) was used to promote the pre-excited molecule to the upper PESs. The combined energy acquired by the molecule, i.e., IR + UV photons, was ∼51150 or ∼53850 $cm^{-1}$ when excited to the second or third overtone, respectively. This energy is well above the dissociation enthalpy, 30173 $cm^{-1}$ (as calculated from the data in refs 25 and 31), for Cl detachment from $CH_3CF_2Cl$, hence causing the excited molecule to dissociate (additional 881 $cm^{-1}$ are needed for Cl* detachment[32]). At the third stage of the experiment, the Cl or Cl* photofragments were detected by (2 + 1) resonantly enhanced multiphoton ionization (REMPI) with the same UV laser pulse used for the electronic excitation.

The experimental setup is the one used in our previous VMP experiments.[2,4,15,17,18] The photodissociation took place in a home-built time-of-flight mass spectrometer (TOFMS)[33] that allowed a sensitive and mass-selective detection. The two

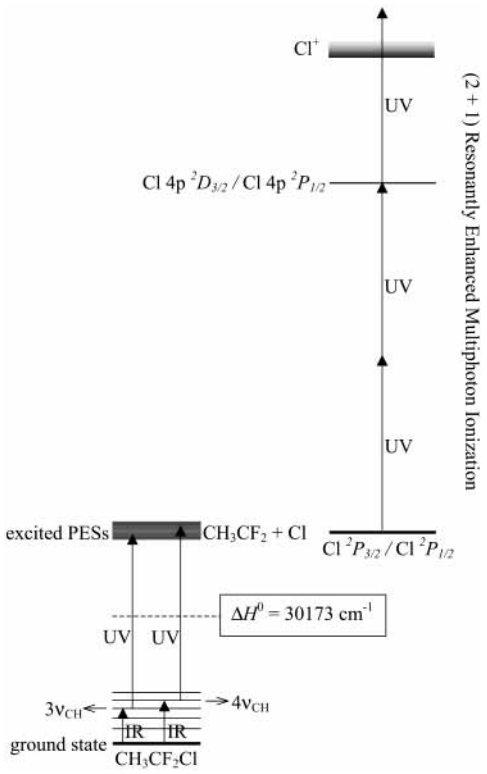


**Figure 1.** Schematics of the experimental concept of vibrationally mediated photodissociation. An IR photon excites the $CH_3CF_2Cl$ molecule to $3\nu_{CH}$ or $4\nu_{CH}$ then a UV photon promotes the molecule to the excited potential energy surfaces (PESs) where the molecule dissociates. The Cl or Cl* photofragments are tagged by the same UV photons via (2 + 1) resonantly enhanced multiphoton ionization. The UV wavelength is 235.336 or 235.205 nm for tagging Cl or Cl*, respectively, according to the corresponding two−photon transitions.

counterpropagating laser beams got into the TOFMS, perpendicular to its axis. The vibrational excitation beam was provided by the idler of an optical parametric oscillator (bandwidth ∼0.08 $cm^{-1}$) that was pumped by the third harmonic output of a Nd:YAG laser. Typical energies of ∼7 and ∼5 mJ were used in the 875−900 and 1140−1180 nm ranges, respectively, and the beam was focused with a 15 cm focal length (f.l.) lens onto the interaction region of the TOFMS. The ∼120 $\mu$J UV beam was delayed by 10−15 ns and focused to the same point with a 30 cm f.l. lens. It was obtained from the doubled output of a tunable dye laser (bandwidth ∼0.5 $cm^{-1}$), pumped by the third harmonic of another Nd:YAG laser. The energies of both lasers were kept at these low values to prevent saturation. Only when both lasers were employed did effective photolysis occur, due to the very low absorption cross section of vibrationless ground-state molecules at ∼235 nm.[25] Pre-excitation of the $CH_3CF_2Cl$ molecules enhanced significantly the photodissociation, owing to a better FC overlap.

The molecular beam was perpendicular to both the TOFMS axis and the laser beams. $CH_3CF_2Cl$ (Atochem, > 99.85%), prepared as a ∼5% mixture in Ar at a total pressure of 760 Torr, was expanded through a pulsed valve and a needle and traveled another ∼2 cm to the chamber center where it was intersected by the laser beams. Two turbomolecular pumps evacuated the source and the ion detector chambers, respectively, and kept a base pressure of $2 \times 10^{-6}$ Torr in both chambers. The pressure increased to $1.6 \times 10^{-5}$ Torr when the pulsed nozzle was on (driven with a pulse of 120 V, ∼190 $\mu$s, 10 Hz). Relying on simulation of the action spectra of the second C−H stretch overtone of propyne-$d_3$, expanded under similar condi-

tions, it is assumed that the expansion resulted in a predominant rotational temperature of ~12 K and a vibrational temperature <100 K.[34]

The photofragments formed in the focal volume were ionized by REMPI via the following two-photon transitions: Cl (4p $^2D_{3/2} \leftarrow$ 3p $^2P_{3/2}$) at 235.336 nm and Cl* (4p $^2P_{1/2} \leftarrow$ 3p $^2P_{1/2}$) at 235.205 nm.[35] Efforts were made to measure also the H signal via the (2s $^2S \leftarrow$ 1s $^2S$) transition at 243.135 nm;[36] however, it was too weak and noisy. The ions were subjected to continuously biased extraction, two acceleration stages, two pairs of orthogonal deflection plates and an Einzel lens prior to entering the field free drift region, and were finally detected by a microsphere plate (MSP) at its end. The MSP output was amplified and fed into a digital oscilloscope and a boxcar integrator where wavelength-dependent ion signals of $^{35}Cl$, $^{37}Cl$, $^{35}Cl^*$, and $^{37}Cl^*$ were captured and processed by a computer. The signals of masses 35 and 37 were monitored simultaneously by two independent boxcar channels, utilizing the mass resolution of the TOFMS. Fixing the UV laser on the wavelength of a particular transition and scanning the IR laser produced action spectrum of the respective photofragment. Each data point in the ensuing spectra was an average of thirty pulses.

The vibrational absorption spectra at room temperature were monitored simultaneously by PA spectroscopy[37] in which an acoustic signal was produced by the relaxation of the vibrationally excited molecules. A dichroic mirror in the IR beam path, after the TOFMS, was used to direct the beam to a PA cell. Wavelength calibration was accomplished by monitoring the rovibrational overtone PA spectra of water in the corresponding wavelength regions and determining the wavelength according to the positions of the water absorption lines taken from the HITRAN database.[38]

In addition, Doppler profiles were measured to determine the Cl*/Cl branching ratios. In these measurements the IR laser was fixed and the UV laser scanned the Cl or Cl* transition. Attention was given to employment of similar experimental conditions in the measurements of Cl and Cl*. The areas of the Gaussian shaped profiles were extracted, and a very small background from the UV one-photon photodissociation was subtracted to get the "net" signal resulting from VMP. The ratio of the experimental areas was corrected with a scaling factor of the above-mentioned transitions[39] to achieve the branching ratio.

## Results and Discussion

**A. PA and Action Spectra.** Figure 2 displays representative PA spectrum (a) and action spectra of $^{35}Cl$ and $^{37}Cl$ (b) and $^{35}Cl^*$ and $^{37}Cl^*$ (c) photofragments, as a function of the excitation laser wavelength scanned across the second $CH_3$ stretch overtone of $CH_3CF_2Cl$. Similar spectra of the third $CH_3$ stretch overtone were measured as well, and those of $^{35}Cl$ and $^{37}Cl$ together with the PA spectrum are given in Figure 3. The PA spectra reflect the contribution of both $CH_3CF_2Cl$ isotopomers, while the $^{35}Cl$ and $^{35}Cl^*$ action spectra account only for the more abundant isotopomer ($CH_3CF_2{}^{35}Cl$, natural abundance ~76%), and the $^{37}Cl$ and $^{37}Cl^*$ action spectra account for the less abundant one ($CH_3CF_2{}^{37}Cl$, ~24%). Nevertheless, the action spectra of all photofragments exhibit a similar structure, and the spectral features corresponding to the $CH_3CF_2Cl$ isotopomers cannot be distinguished under our resolution, similarly to the situation encountered in $CH_3CFCl_2$.[4] On the other hand, the action spectra of $CHF_2Cl$ and $CHFCl_2$ exhibited narrower features, enabling observation of a shift between the peaks of the different isotopomers, yet, the general appearance

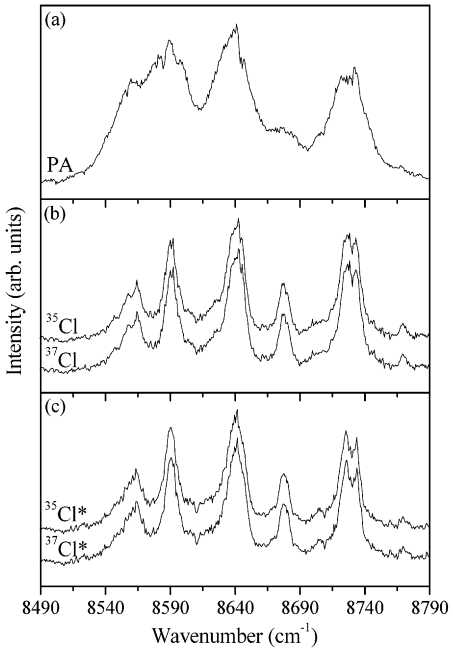


**Figure 2.** Vibrational overtone excitation spectra of $3\nu_{CH}$ of $CH_3CF_2Cl$. (a) Photoacoustic absorption spectrum. (b) $^{35}Cl$ and $^{37}Cl$ action spectra. (c) $^{35}Cl^*$ and $^{37}Cl^*$ action spectra.

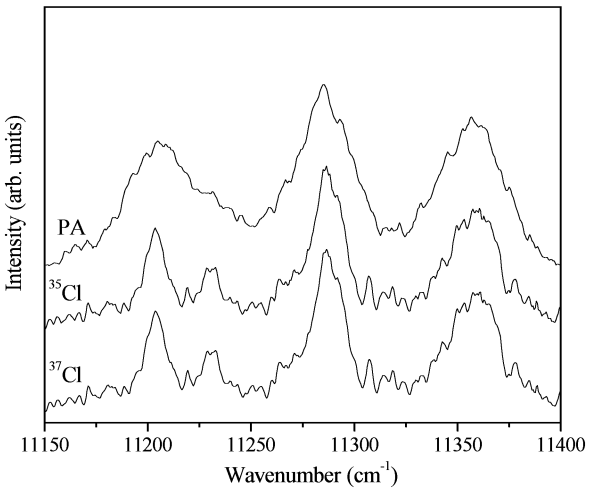


**Figure 3.** Vibrational overtone excitation spectra of $4\nu_{CH}$ of $CH_3CF_2Cl$: photoacoustic absorption spectrum and $^{35}Cl$ and $^{37}Cl$ action spectra.

of the features and the relative intensities between the different bands were similar in all the action spectra.[15,17] Contrasting behavior was found in VMP of $CH_3Cl$ pre-excited with three quanta of C−H stretch,[9] where the action spectra of $^{35}Cl^*$ and $^{37}Cl^*$ differed. Moreover, the intensities of the bands in the PA and action spectra of $CH_3Cl$ differed, and the $\nu_1 + 2\nu_4$ band was absent in the latter, implying that the cross sections for VMP via the second C−H stretch overtone depend on the specific excited vibrational level.

Both the PA and action spectra of the second and third overtones of $CH_3CF_2Cl$ are characterized by multiple peak structure. A similar multiple peak structure was found aso in the second and third $CH_3$ overtone spectra of $CH_3CFCl_2$ (refs 4 and 29) and was attributed, in both cases, to coupling between the $CH_3$ stretches and deformations. To support this ascription we applied the simplified LM model,[29] relying on Duncan et al.[30] The model accounts for the C−H stretch modes, Darling−Dennison resonances between them, and stretch−deformation Fermi resonances, and its results pointed to multiple peak

**TABLE 1: Spectral Spacing between Stretch−Bend Mixed States and between the Mixed States and Close Lying Resonant Dark States, and the Corresponding Time Scales for Energy Redistribution**

| | mixed states | | local resonances between mixed and dark states | | | |
|---|---|---|---|---|---|---|
| molecule | $\Delta\nu$ ($cm^{-1}$) | $\tau$ (ps) | peak 1 ($cm^{-1}$) | peak 2 ($cm^{-1}$) | $\tau$ (ps) | refs |
| $CH_3CF_2Cl$[a] | 28−71 | 0.25−0.60 | 8726.5 | 8734 | 2.2 | this work |
| $CH_3CFCl_2$[a] | 25−60 | 0.25−0.65 | 11328 | 11346 | 0.9 | 4 |
| $CHFCl_2$[b] | 150−260 | 0.05−0.10 | 9975 | 9988 | 1.3 | 15 |
| $CHF_2Cl$[b] | 100−210 | 0.08−0.17 | 8725 | 8718.5 | 2.6 | 17 |
| | | | 8457 | 8469 | 1.4 | 17 |
| | | | 11429.5 | 11427.5 | 8.8 | 17 |
| | | | 11200 | 11222.5 | 0.7 | 17 |
| $CHCl_3$ | | $\sim 0.05$[c] | 11382.5 | 11386.5 | $\sim 5$ | 47 |
| $CHF_3$ | | $< 0.10$[c] | 13800 | 13807 | $\sim 2.5$ | 13, 46 |

[a] The data are for the $3\nu_{CH}$ and $4\nu_{CH}$ bands. [b] The data are for the $N = 3$, 7/2 and 4 polyads. [c] These values were calculated using the effective Hamiltonian and the time evolution matrix (ref 46).

structures of mixed stretch−deformation eigenstates in the corresponding spectral regions, in accordance with the observations.

The jet-cooled action spectra and the room temperature PA spectra differ mainly by their peak widths (Figures 2 and 3). In the former, most of the peaks are 40−60% narrower and therefore more resolved. Due to the better resolution, the shoulders observed at the low-frequency end of both $3\nu_{CH}$ and $4\nu_{CH}$ manifolds and at $\sim$8670 $cm^{-1}$ in the $3\nu_{CH}$ region of the PA spectra appear as resolved peaks in the action spectra. Another prominent difference between the PA and action spectra is that the peak of highest frequency in the second overtone region is split into two peaks in the latter.

The line widths of the observed overtone spectra are determined by both homogeneous and inhomogeneous contributions. The inhomogeneous structure is influenced mainly by the width of the rotational contour of the transition and by the overlap with hot band transitions. $CH_3CF_2Cl$ has a few low-frequency vibrational modes,[40] which at room temperature occupy $\sim$52% of the population. Hence, it is reasonable that hot bands underlying the corresponding overtone regions contribute to the observed PA spectral structure. Indeed, the low-frequency peak of $4\nu_{CH}$ possesses the largest area in the PA spectrum but is much smaller than other peaks in the action spectra, demonstrating the existence of hot bands in this spectral region. Another source for the peak widths might be the existence of several conformers. $CH_3CF_2Cl$ possesses two conformers, staggered and eclipsed, where the energy of the latter is 3.7−4.4 kcal $mol^{-1}$ higher than that of the former.[31,41] The probability to overcome a barrier of this height in vibrationless ground-state molecules even at room temperature is low; however, it may be that the vibrational excitation induces conformational isomerization as in the case of 2-fluoroethanol excited to the $-CH_2F$ asymmetric C−H stretch.[42]

The inhomogeneous contribution is significantly reduced in the jet-cooled action spectra. Most of the vibrational and some of the rotational congestion is eliminated at rotational temperature of $\sim$12 K and vibrational temperature <100 K. Therefore, the jet-cooled action spectra reveal more of the homogeneous structure that reflects the vibrational couplings of the mixed stretch−deformation states among themselves and with other modes of the molecule. The appearance of several peaks in the frequency domain, caused by the strong coupling between stretch and deformation modes, is exhibited in the time domain by quantum beats,[43] i.e., a periodic return of the vibrational energy to the excited mode, with a recurrence period $\tau = 1/c\Delta\nu$, where $\Delta\nu$ is the spectral splitting between the states.[13] The splittings in the C−H overtone spectra of $CH_3CF_2Cl$ and some other compounds, together with the corresponding energy redistribution time scales, i.e., half the periods, are given in Table 1. As can be seen, similar time scales were found for the second and third overtones of both $CH_3CF_2Cl$ and $CH_3CFCl_2$, where the redistribution time between the stretch-deformation mixed states was estimated as 0.25−0.65 ps.

Nevertheless, the situation is somewhat different for molecules with an isolated C−H chromophore where, as shown in Table 1, the energy redistribution between C−H stretches and bends usually takes less than 0.1 ps, and in the extreme cases less than 0.2 ps. In these molecules the spectra were characterized by polyads of many components separated by hundreds of wavenumbers in each C−H overtone region, which were attributed to stretch−bend coupling and were analyzed by Quack and co-workers by a normal-mode model.[44−46] They also calculated the time evolution of the zero-order states,[46] and the redistribution time between the C−H stretching and bends was assessed around 0.03−0.10 ps.[47,48] We applied jet-cooled action spectroscopy to study the second and third stretch−bend overtones of the methane derivatives homologues of $CH_3CF_2Cl$ and $CH_3CFCl_2$, i.e., $CHF_2Cl$ and $CHFCl_2$, and found that the redistribution between the mixed states occurs within 0.05−0.17 ps.[15,17] These findings indicate that the energy redistribution in the methyl group of $CH_3CF_2Cl$ and $CH_3CFCl_2$ is slower than in the molecules with isolated C−H chromophore. The apparent redistribution reflects the mixing of stretches and deformations via Fermi resonance. Also, these resonances have an important role in IVR of other methyl-containing molecules such as the isotopomers of toluene, where the influence of stretch−bend interaction changes for the different overtones, as they tune in and out resonance.[49]

An interesting feature of the action spectra is the splitting in the highest frequency peak of the $3\nu_{CH}$ region into two peaks, one at 8734.0 $cm^{-1}$ and the other at 8726.5 $cm^{-1}$. The splitting may arise from a local resonance between the mixed stretch−deformation eigenstate and another close lying state. The energies of the unperturbed states and the coupling constant, $W$, may be found by the two-level model,[50] using the known energies of the perturbed states and their relative intensities. The energies were determined as $8733 \pm 1$ and $8727.5 \pm 1$ $cm^{-1}$ and the coupling constant $|W| = 2.6$ $cm^{-1}$; however, the resonant dark state could not be definitely identified due to the large number of possible combination bands with comparable energy.

A similar phenomenon of peak splitting resulting from local resonances appears in other HCFCs and also in other C−H containing molecules. Some examples for these splittings together with the corresponding time scales for energy redistribution between the resonating mixed and dark states are given in Table 1 (the oscillation period is given by $\tau = 1/c\Delta\nu$, as

**TABLE 2: Cl*/Cl Branching Ratios in Vibrationless Ground State and Vibrationally Mediated Photodissociation of $CH_3CF_2Cl$, $CH_3CFCl_2$, $CHF_2Cl$, and $CHFCl_2$**

| | direct photodissociation | | vibrationally mediated photodissociation | | |
|---|---|---|---|---|---|
| | 193 nm | refs | 2nd overtone | 3rd overtone | refs |
| energy[a] | 51813 | | ~ 51150 | ~ 53850 | |
| $CH_3CF_2Cl$ | $0.25 \pm 0.06$[b] | 7, 28 | $0.54 \pm 0.09$ | $0.55 \pm 0.09$ | this work |
| | $0.39 \pm 0.11$[c] | 51 | | | |
| $CH_3CFCl_2$ | $0.22 \pm 0.06$[b] | 7, 28 | $0.49 \pm 0.11$ | $0.46 \pm 0.10$ | 4 |
| $CHF_2Cl$ | $0.50 \pm 0.04$[b] | 7, 27 | $0.55 \pm 0.09$ | $0.50 \pm 0.09$ | 17 |
| $CHFCl_2$ | | | $0.52 \pm 0.13$ | $0.49 \pm 0.10$ | 15 |

[a] The energy given for VMP is the combined energy, vibrational excitation + photodissociation, differing somewhat for each compound according to the monitored eigenstate. [b] The value differs from that given in the refs, due to different scaling factors used. [c] This ratio was measured at room temperature, whereas all the other values are for jet-cooled samples.

explained above). It is clearly seen from Table 1 that the recurrence time differs from molecule to molecule and even for different bands of the same molecule, yet the separation of the split peaks is always smaller than the splitting between the mixed states implying a longer redistribution time. This manifests the existence of two time scales for IVR, the shorter one between the strongly coupled mixed states and the longer one between them and the rest of the molecule via the local resonances.

**B. Branching Ratios.** The emergence of the action spectrum means that the yield of the monitored photofragment is enhanced by the vibrational excitation. This enhancement was observed for all the photofragments we probed (i.e., H, Cl, and Cl*); nevertheless, it was less extensive for H. The enhancement of the Cl and Cl* yield when the C−H methyl stretch is excited before photodissociation might indicate the intramolecular energy flow to the C−Cl bond, which becomes the reaction coordinate. As metioned above, IVR occurs in less than one ps whereas the laser pulse durations and the delay between them are a few ns; hence, when photodissociation takes place energy has already been redistributed. The photofragment yield is dependent on the vibrational excitation efficiency, the absorption from the vibrational state to the upper electronic states, and the branching into the specific channel. The fact that H photofragment signal was enhanced to a lesser extent than the chlorine photofragment implies IVR to the C−Cl bond and, probably, a better FC overlap of vibrational modes containing C−Cl excitation and a higher electronic transition probability to the upper PESs.

Moreover, additional information regarding the dynamics on the upper PESs may be provided by the branching ratios of the photoproducts. The branching ratios were calculated from the Doppler profiles corrected by a scaling factor of the REMPI transitions.[39] The Cl*/Cl branching ratios for $CH_3CF_2Cl$ VMP via the second and third C−H methyl overtones are presented in Table 2 together with the branching ratio for 193 nm vibrationless ground-state photodissociation. Also given in the table are the Cl*/Cl ratios for photodissociation of $CH_3CFCl_2$, $CHF_2Cl$, and $CHFCl_2$. It is worth noting that the 193 nm branching ratios were corrected for the new available transition probabilities.[35,39,51] As shown in Table 2, the branching ratios in VMP are about 0.5 for all the compounds. Nevertheless, in 193 nm direct photodissociation there is a clear difference between $CHF_2Cl$ and the ethane derivatives: while the former has a Cl*/Cl ratio of 0.5, the latter possess considerably lower values. The energy of the 193 nm photon (51813 $cm^{-1}$) falls between the combined energies used for VMP of $CH_3CF_2Cl$ and $CH_3CFCl_2$ via $3\nu_{CH}$ and $4\nu_{CH}$ (see Table 2). Therefore, the alteration of the branching ratio in VMP of $CH_3CF_2Cl$ and $CH_3CFCl_2$, as compared to the almost isoenergetic vibrationless ground-state photodissociation, implies that the dynamics of the photolysis is varied. The same trend is exhibited also by the different Cl*/Cl branching ratios for vibrationless ground state 193 nm photodissociation of $CH_3CF_2Cl$ at room temperature obtained by Brownsword et al. from laser induced fluoroscence (LIF) tagging of Cl and Cl* combined with a photolytic calibration method.[52] They found a higher branching ratio than that for the cooled molecules and lower than for VMP. This might be because the dissociation occurs partly via vibrationally excited states, since, as mentioned above, at room temperature 52% of the molecules are vibrationally excited.

These four HCFC compounds belong to the $C_s$ symmetry group and may have transitions to states of A′ and A″ symmetries (for $CHF^{35}Cl^{37}Cl$ and $CH_3CF^{35}Cl^{37}Cl$ the symmetry reduces to $C_1$). However, $CHFCl_2$ and $CH_3CFCl_2$ possess two Cl atoms lying in the symmetry plane, whereas in $CHF_2Cl$ and $CH_3CF_2Cl$ the C−Cl bond is out of the symmetry plane. The different branching ratios at 193 nm photodissociation of the different molecules led us to infer that at least two PESs of different symmetries are involved in the absorption.[28] Indeed, Ying and Leung[53] have shown by molecular orbital calculations that transitions of both symmetries underlie the first absorption band of $CHF_2Cl$ and $CHFCl_2$, related to the $\sigma^* \leftarrow n$ transition. In the former, two transitions are involved with predominance of the A′ ← A′, while in the latter four transitions are possible where only two of them contribute substantially, dominated by the lowest A″ ← A′. Accordingly, it is reasonable that Cl and Cl* are formed in direct and vibrationally mediated photodissociation of these molecules via absorption to A′ and A″ states followed by curve crossing as the fragments depart from the molecule.[54] Also, measurements of the anisotropy parameter, $\beta$, in VMP of $CHFCl_2$ and $CH_3CFCl_2$, excited in the second and third C−H overtone regions,[18,19] revealed positive values, similar for both Cl and Cl*, and lower than the limiting value for a pure A″ ← A′ transition. This together with the Cl*/Cl branching ratios indicate that both Cl and Cl* are produced in these cases by simultaneous absorption to A′ and A″ states that probably mix via curve crossing. A positive $\beta$ was found in the 193 nm photodissociation of $CHFCl_2$ as well, and was attributed also there to the involvement of two transitions.[55] The resemblance in structure and branching ratios leads us to infer that also in photodissociation of $CH_3CF_2Cl$ at least two states of different symmetries are involved and the Cl*/Cl branching ratio is determined by the nonadiabatic interplay between them. The increase of the Cl*/Cl ratio in VMP of $CH_3CF_2Cl$ and $CH_3CF_2Cl$ as compared to the vibrationless ground-state photodissociation indicates that the nonadiabatic processes are more dominant in the former case. Another possibility is that the accessibility of the various PESs is changed due to the vibrational excitation. A similar phenomenon of increase in the branching into Cl* was observed in VMP of $CH_3Cl$ and $CHD_2Cl$ pre-excited to the fourth overtone of the C−H stretch, with

a larger increase in $CH_3Cl$.[6,8] In the photodissociation of vibrationally excited $CF_3I$ (prepared by heating the sample) an increase in the branching into I photoproducts was found.[5] The alteration of branching ratio in all the above-mentioned compounds demonstrates the effect of vibrational pre-excitation of the alkyl group on the photodissociation dynamics, presumably due to further crossing between the upper PESs.

## Conclusions

The action spectra of the $3\nu_{CH}$ and $4\nu_{CH}$ regions of $CH_3CF_2Cl$, obtained by VMP of jet-cooled samples, exhibit multipeak structures attributed to mixed eigenstates of methyl stretch and deformation. The action spectra resemble the PA spectra of the same spectral regions; however, they are narrower and, due to their better resolution, a new feature is revealed in the region of the highest frequency peak of the second overtone. This feature is related to a local resonance of the stretch−deformation eigenstate with a neighboring dark state, and the splitting between them reflects a redistribution time, ~2 ps, that is larger than the 0.3−0.6 ps redistribution time between the stretch−deformation states. The energy flow from the C−H to the C−Cl bond is also manifested by the increased yield of chlorine photofragments, in both ground and spin−orbit excited states, that presumably results from a better FC overlap with the upper PESs and a higher electronic transition probability. The Cl*/Cl branching ratios are ~0.5, very similar to those of $CH_3CFCl_2$, therefore it is inferred that also in this case the photodissociation involves at least two transitions to states of A′ and A″ symmetries and the branching ratio is determined by the nonadiabatic interactions between them.

**Acknowledgment.** We thank Professor P. J. Dagdigian for useful discussions. This research was supported by grant No. 99-00044 from the United States−Israel Binational Foundation (BSF), and by the James Franck Binational German−Israeli Program in Laser-Matter Interaction.

## References and Notes

(1) Crim, F. F. *J. Phys. Chem.* **1996**, *100*, 12725.
(2) Bar, I.; Rosenwaks, S. *Int. Rev. Phys. Chem.* **2001**, *20*, 711.
(3) Melchior, A.; Chen, X.; Bar, I.; Rosenwaks, S. *Chem. Phys. Lett.* **1999**, *315*, 421.
(4) Melchior, A.; Chen, X.; Bar, I.; Rosenwaks, S. *J. Chem. Phys.* **2000**, *112*, 10787.
(5) Person, M. D.;. Kash, P. W; Butler, L. J. *J. Chem. Phys.* **1991**, *94*, 2557.
(6) Lambert, H. M.; Dagdigian, P. J. *Chem. Phys. Lett.* **1997**, *275*, 499.
(7) Melchior, A.; Lambert, H. M.; Dagdigian, P. J.; Bar, I.; Rosenwaks, S. *Isr. J. Chem.* **1997**, *37*, 455.
(8) Lambert, H. M.; Dagdigian, P. J. *J. Chem. Phys.* **1998**, *109*, 7810.
(9) Tao, C.; Dagdigian, P. J. *Chem. Phys. Lett.* **2001**, *350*, 63.
(10) Zhang, J.; Dulligan, M.; Wittig, C. *J. Phys. Chem.* **1995**, *99*, 7446.
(11) Berghout, H. L.; Brown, S. S.; Delgado, R.; Crim, F. F. *J. Chem. Phys.* **1998**, *109*, 2257.
(12) (a) Schmid, R. P.; Arusi-Parpar, T.; Li, R,-J.; Bar, I.; Rosenwaks, S. *J. Chem. Phys.* **1997**, *107*, 385. (b) Schmid, R. P.; Ganot, Y.; Bar, I.; Rosenwaks, S. *J. Chem. Phys.* **1998**, *109*, 8959.
(13) Boyarkin, O. V.; Settle, R. D. F.; Rizzo, T. R. *Ber Bunsen-Ges. Phys. Chem.* **1995**, *99*, 504.
(14) Boyarkin, O. V.; Lubich, L.; Settle, R. D. F.; Perry, D. S.; Rizzo, T. R. *J. Chem. Phys.* **1997**, *107*, 8409. Boyarkin, O. V.; Rizzo, T. R.; Perry, D. S. *J. Chem. Phys.* **1999**, *110*, 11346. Chirokolava, A.; Perry, D. S.; Boyarkin, O. V.; Schmid, M.; Rizzo, T. R. *J. Chem. Phys.* **2000**, *113*, 10068.
(15) Melchior, A.; Chen, X.; Bar, I.; Rosenwaks, S. *J. Phys. Chem. A* **2000**, *104*, 7927.
(16) Coffey, M. J.; Berghout, H. L.; Woods, E.; Crim, F. F. *J. Chem. Phys.* **1999**, *110*, 10850.
(17) Li, L.; Dorfman, G.; Melchior, A.; Rosenwaks, S.; Bar, I. *J. Chem. Phys.* **2002**, *116*, 1869.
(18) Chen, X.; Marom, R.; Rosenwaks, S.; Bar, I.; Einfeld, T.; Maul, C.; Gericke, K.-H. *J. Chem. Phys.* **2001**, *114*, 9033.
(19) Einfeld, T.; Maul, C.; Gericke, K.-H.; Marom, R.; Rosenwaks, S.; Bar, I. *J. Chem. Phys.* **2001**, *115*, 6418.
(20) Rowland, F. S. *Environ. Sci. Technol.* **1991**, *25*, 622.
(21) McFarland, M.; Kaye, J. *Photochem. Photobiol.* **1992**, *55*, 911.
(22) Scientific Assessment of Ozone Depletion: 1991. World Meteorological Organization Global Research and Monitoring Project Report No. 25; World Meteorological Organization: Geneva, Switzerland, 1992.
(23) Robin, M. B. *Can. J. Chem.* **1985**, *63*, 2032.
(24) Fahr, A.; Braun, W.; Kurylo, M. J. *J. Geophys. Res.* **1993**, *98*, 20467.
(25) Atkinson, R.; Baulch, D. L.; Cox, R. A.; Hampson, R. F., Jr.; Kerr, J. A.; Troe, J. *J. Phys. Chem. Ref. Data* **1992**, *21*, 1125.
(26) Hubrich, C.; Zetzsch, C.; Stuhl, F. *Ber. Bunsen-Ges. Phys. Chem.* **1977**, *81*, 437.
(27) Melchior, A.; Knupfer, P.; Bar, I.; Rosenwaks, S.; Laurent, T.; Volpp, H.-R.; Wolfrum, J. *J. Phys. Chem.* **1996**, *100*, 13375.
(28) Melchior, A.; Bar, I.; Rosenwaks, S. *J. Chem. Phys.* **1997**, *107*, 8476.
(29) Chen, X.; Melchior, A.; Bar, I.; Rosenwaks, S. *J. Chem. Phys.* **2000**, *112*, 4111.
(30) Duncan, J. L.; New, C. A.; Leavitt, B. *J. Chem. Phys.* **1995**, *102*, 4012.
(31) Paddison, S. J.; Chen, Y.; Tschuikow-Roux, E. *Can. J. Chem.* **1994**, *72*, 561.
(32) Okabe H. *Photochemistry of Small Molecules*; John Wiley & Sons: New York, 1978.
(33) Wiley, W. C.; McLaren, I. H. *Rev. Sci. Instrum.* **1955**, *26*, 1150.
(34) Chen, X.; Ganot, Y.; Bar, I.; Rosenwaks, S. *J. Chem. Phys.* **2000**, *113*, 5134.
(35) Liyanage, R.; Yang, Y.; Hashimoto, S.; Gordon, R. J.; Field, R. W. *J. Chem. Phys.* **1995**, *103*, 6811.
(36) Matsumi, Y.; Tonokura, K.; Kawasaki, M.; Tsuji, K.; Obi, K. *J. Chem. Phys.* **1993**, *98*, 8330.
(37) West, G. A.; Barrett, J. J.; Siebert, D. R.; Reddy, K. V. *Rev. Sci. Instrum.* **1983**, *54*, 797.
(38) Rothman, L. S.; Rinsland, C. P.; Goldman, A.; Massie, S. T.; Edwards, D. P.; Flaud, J.-M.; Perrin, A.; Camy-Peyret, C.; Dana, V.; Mandin, J.-Y.; Schroeder, J.; McCann, A.; Gamache, R. R.; Wattson, R. B.; Yoshino, K.; Chance, K. V.; Jucks, K. W.; Brown, L. R.; Nemtchinov, V.; Varanasi, P. "*The 1996 HITRAN Molecular Spectroscopic Database and HAWKS* (HITRAN Atmospheric Workstation)". *J. Quant. Spectrosc. Radiat. Transfer* **1998**, *60*, 665.
(39) Regan, P. M.; Langford, S. R.; Ascenzi, D.; Cook, P. A.; Orr-Ewing, A. J.; Ashfold, M. N. R. *Phys. Chem. Chem. Phys.* **1999**, *1*, 3247.
(40) McNaughton, D.; Evans, C. *J. Mol. Spectrosc.* **1997**, *182*, 342.
(41) Durig, J. R.; Bucy, W. E.; Wurrey, C. J. *J. Chem. Phys.* **1974**, *60*, 3293.
(42) Hudspeth, E.; McWhorter, D. A.; Pate, B. H. *J. Chem. Phys.* **1997**, *107*, 8189.
(43) Felker, P. M.; Zewail, A. H. *J. Chem. Phys.* **1985**, *82*, 2994.
(44) Amrein, A.; Dubal, H.-R.; Quack, M. *Mol. Phys.* **1985**, *56*, 727.
(45) Dubal, H.-R.; Quack, M. *Mol. Phys.* **1984**, *53*, 257.
(46) Dubal, H.-R.; Quack, M. *J. Chem. Phys.* **1984**, *81*, 3779.
(47) Hippler, M.; Quack, M. *J. Chem. Phys.* **1996**, *104*, 7426.
(48) Hippler, M.; Quack, M. *Ber. Bunsen-Ges. Phys. Chem.* **1997**, *101*, 356.
(49) Cavagnat, D.; Lespade, L. *J. Chem. Phys.* **2001**, *114*, 6030, *ibid* 6041.
(50) Herzberg, G. *Molecular Spectra and Molecular Structure. II Infrared and Raman Spectra of Polyatomic Molecules*; Van Nostrand Reinhold Co.; New York, 1945.
(51) Matsumi, Y.; Tonokura, K.; Kawasaki, M.; Inoue, G.; Satyapal, S.; Bersohn, R. *J. Chem. Phys.* **1992**, *97*, 5261.
(52) Brownsword, R. A.; Schmiechen, P.; Volpp, H.-R.; Upadhyaya, H. P.; Jung, Y. J.; Jung, K.-H. *J. Chem. Phys.* **1999**, *110*, 11823.
(53) Ying, J. F.; Leung, K. T. *J. Chem. Phys.* **1996**, *105*, 2188.
(54) Lambert, H. M.; Dagdigian, P. J.; Alexander, M. H. *J. Chem. Phys.* **1998**, *108*, 4460.
(55) Yang, X.; Felder, P.; Huber, R. J. *Chem. Phys.* **1994**, *189*, 124.